kw: Simulation; Applications; Batteries; Cost; Energy; Reliability; Variation; Operation
class: Energy

(1729)

RERIC International Energy Journal: Vol. 12, No. 1, June 1990 p. 21 – 39

The Sizing of Stand-alone Photovoltaic Systems Using the Simulation Technique

France Lasnier and Wang Yaw Juen
Energy Technology Division
Asian Institute of Technology
Bangkok 10501
Thailand

ABSTRACT

The application of the simulation technique in photovoltaic (PV) system sizing is presented in this paper. Simulation of a PV system of several array sizes and battery capacities gives the relationship between system reliability (loss of load hours, LOLH) and system size (array and battery). Through the relationship, optimum combinations of array and battery sizes to meet prescribed reliabilities are first determined. Since a low level of reliability requires less system investment but incurs a resultant outage cost (i.e. the cost to energy consumers of running an auxiliary system if the PV system is unable to supply energy) an economic evaluation of backup power (a diesel generator) and investment in arrays and batteries must be made to determine the optimum system reliability so that the array and battery size to meet the reliability, and the expected number of backup power running hours can be obtained. This paper also discusses the effect of load pattern on sizing, variation of loss of load frequencies (LOLF) with array-battery combinations leading to the same LOLH value, and different battery operations (deep/shallow cycle) arising from different array-battery combinations.

INTRODUCTION

The primary concern in designing any PV system is the determination of its optimum size. It is generally inadequate to use monthly or daily average insolation, and estimated number of continuous "no sun" days to determine array and battery capacities because the dynamic behavior of a PV system and the stochastic nature of solar radiation also significantly influence the required array and storage capacity. The simulation method uses hourly meteorological data and hourly load data to simulate the energy flow in a PV system, and predicts the system reliabilities under assumed array and battery sizes. The simulation thus provides the reliability-array-battery relationship in a discontinuous form. Through numerical methods, one can formulate the discrete relationship into an analytical form. One can also find that there exists several combinations of array and battery sizes to meet a desired reliability (the substitution nature between array and battery). The first problem of sizing is thus to find the optimum combination which minimizes energy costs at a chosen reliability.

Because a PV system with perfect reliability is oversized to meet a relatively low percentage of time when it is faced with peak load and/or cloudy days, it is usually more expensive to size a PV system with perfect reliability than to add backup power which may cover the energy shortage due to unavailability of sunshine. Accordingly, the second problem of sizing is to evaluate the

trade-off between system reliability and the cost of running a backup power for a given number of hours (outage cost).

This paper chooses the loss of load hours (LOLH) as the system reliability index, and considers a residential system which consumes 2 kWh of electricity per day, as a case study. The meteorological data for the simulation are based on data in Thailand.

MODELLING OF SYSTEM COMPONENTS

The system block diagram is shown in Fig. 1. Each block represents a subsystem. It consists of array, battery, charge regulator and generator. Insolation, ambient temperature, and load consumption profile are the factors which influence the performance of the system. Mathematical models for each subsystem are described briefly below:

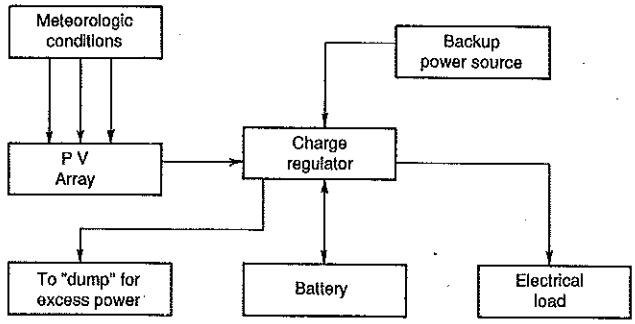

Fig. 1. Scheme of a stand-alone PV system.

Solar Radiation Database

In order to reduce the required computation time, the radiation database used for the simulation is the hourly typical global radiation over one year. The source of the solar radiation database was generated by the "RAMP 1.0" software [1]. The software can simulate the hourly global radiation onto a tilted plane over a specified period. The solar radiation model used in RAMP 1.0 is a binomial distribution radiation model based on data collected in Thailand [2].

Ambient Temperature Model

The sinusoidal ambient temperature model, which involves the maximum and the minimum ambient temperature in a day, is employed:

$$T_a(t) = [(T_{max} + T_{min}) + (T_{max} - T_{min}) \sin(wt)] / 2 \quad (1)$$

where $T_a(t)$ = the ambient temperature at time t
T_{max} = the maximum ambient temperature of the day
T_{min} = the minimum ambient temperature of the day
w = $2\pi/24$

Assuming that the minimum ambient temperature is at 03:00 and the maximum ambient temperature occurs at 15:00, $t = hr - 9$ is taken in Eq. (1) where *hr* is the time (in hours) of interest. The seasonal variations of T_{max} and T_{min} are considered by dividing a year into 8 periods during which average T_{max} and T_{min} are taken [3]. Table 1 lists the temperature variations for eight periods in Thailand.

Table 1. Average maximum and minimum ambient temperature (°C) in 8 periods in Thailand.

Period	Range	Ambient Temperature	
		T_{max}	T_{min}
1	Jan. 14 - Feb. 26	33.3	21.8
2	Feb. 27 - Apr. 12	35.6	23.5
3	Apr. 13 - May. 28	35.5	24.9
4	May. 29 - Jul. 15	33.9	25.1
5	Jul. 16 - Aug. 31	32.8	24.9
6	Sep. 1 - Oct. 15	32.6	24.9
7	Oct. 16 - Nov. 29	31.9	23.6
8	Nov. 30 - Jan. 1	32.1	21.1

Array I-V Model

The PV array is divided into modules which are connected in parallel. The I-V characteristics of each module are represented by an equation of the form [4]:

$$I = I_{sc}[1 - C_1\{\exp(V/(C_2V_{oc})) - 1\}] \tag{2}$$

at a given cell temperature T_{co}, and insolation L_o

where
$$C_1 = (1 - I_{mp}/I_{sc}) \exp[-V_{mp}/(C_2V_{oc})] \tag{3}$$
$$C_2 = (V_{mp}/V_{oc} - 1)/\text{Ln}(1 - I_{mp}/I_{sc}) \tag{4}$$

I = module current, amps
I_{mp} = module maximum power current, amps
I_{sc} = module short-circuit current, amps
V = module voltage, volts
V_{mp} = module maximum power voltage, volts
V_{oc} = module open-circuit voltage, volts.

To obtain the I-V curves at insolation L, and cell temperature T_c, the following transformations are applied:

$$I_{new} = I + \alpha(T_c - T_{co}) + (L/L_o - 1)I_{sc} \tag{5}$$

$$V_{new} = V + \beta(T_c - T_{co}) \tag{6}$$

where

$$\alpha = \frac{\delta I_{sc}}{\delta T} \Big| L = cnst$$

$$\beta = \frac{\delta V_{oc}}{\delta T} \Big| L = cnst$$

α and β are the temperature coefficients for I_{sc} and V_{oc} respectively.

Array Temperature Model

A simple empirical model is used to estimate array temperature from insolation, ambient temperature and wind speed [5]:

$$T_c = T_a + \theta_I \ (1 + \theta_T T_a) (1 - \theta_w V_w) \ \phi$$

where T_c = the array temperature, °C
T_a = the ambient temperature, °C
V_w = the wind speed, m/sec
ϕ = the incident solar insolation, W/m²
θ_I, θ_T and θ_w are constants and are determined by experimental data.

In this model, radiative and convective losses are considered approximately linear with the temperature differing with the ambiance because air does not absorb a significant amount of radiant energy; most heat transferred from the array surface is by convection.

In this paper, θ_I = 0.0138, θ_T = 0.031 and θ_w = 0.042 are used. Wind speed is taken as a constant equal to 1 m/sec to facilitate the model. Further, a correction coefficient, (1 – 1.055 o), where o is the array efficiency, may be introduced into Eq. (7) to allow for the effect of electricity output.

Load Model

Three different daily load profiles are selected to be supplied with photovoltaic electricity. These profiles are hourly defined and the yearly electric consumption value is kept constant. Figure 2 shows these three profiles; constant demand, constant demand with a peak and cosine function profile [6]. In the simulation program, the user may specify three values:

(1) daily energy consumption, E (kWh).
(2) ratio of peak demand to the lowest demand, K.
(3) the time at which the peak demand happens, t_p (hr).

In this paper E = 2, K = 10 and t_p = 12 are the specified values for the sizing case study. The mathematical formulae for each profile are as follows:

The constant demand model

$$D(t) = E/24 \ D_o \qquad (8)$$

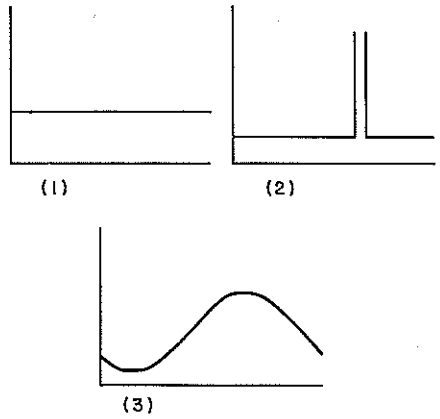

Fig. 2. Load models:
no. (1): Constant demand
no. (2): Constant demand with a peak
no. (3): Demand in cosine function.

The constant demand with one peak

$$D(t) = \begin{cases} KE/(23+K), & \text{when } t = t_p \\ E/(23+K), & \text{when } t \neq t_p \end{cases} \quad (9)$$

The cosine function model

$$D(t) = D_o + D_m \cos [2\pi (t - t_p)/24] \quad (10)$$

$$D_m = D_o (K-1)/(K+1) \quad (11)$$

where D_m is the amplitude of the cosine function.

Profile no. 1 is taken as the sizing case study, and profile no. 2 and no. 3 are used to investigate the effect of load patterns and peak time t_p on sizing.

Charge Regulator

A charge regulator is used to despatch energy flow among arrays, batteries and loads. The first priority is to prevent batteries from over charge and deep discharge.

Assuming that the loads consume DC power only, power flow controlled by the charge regulator is arranged so that the array energy is first used to meet the load and any excess is stored in the batteries. If batteries are full, the excess is "dumped" by dissipating the electrical power in a resistive network. If the load cannot be met by the array alone, the difference is requested from the batteries. When the battery's state of charge (SOC) drops to the minimum permitted value, e.g. 30% of the capacity, the regulator disconnects the load. The duration of the load disconnection is then recorded as loss of load hours (LOLH) and such an event is a loss of load event (LOLE)

which is accumulated over a specified duration, e.g. one year, to be a loss of load frequency (LOLF) (Fig. 3).

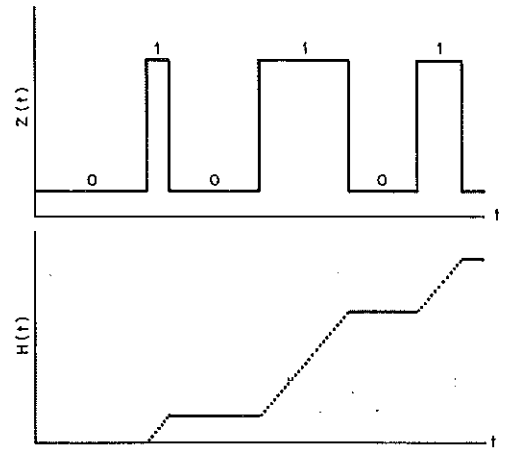

Fig. 3. Loss of load event $Z(t)$ and loss of load hours $H(t)$.

Battery Model

A battery model considering internal charge/discharge resistance is employed to calculate the battery state of charge (SOC). The battery SOC at $(t + dt)$ can be estimated from the present SOC by computing the energy input (output), battery self-discharge and losses [7].

$$S_{t+dt} = S_t (1 - D_s\, dt) + K_1 (V I_b - K_2 I_b^2)\, dt \tag{12}$$

where
S_t = battery state of charge at time t, Wh
D_s = battery self-discharge rate, W
K_1 = battery charge/discharge efficiency
K_2 = battery charge/discharge resistance, ohm
V = system voltage, volts
I_b = battery current, amps.

The battery charge/discharge voltage and resistances are also updated every dt according to Eq. (13):

$$\begin{aligned} R_2 &= S_{bal}/S_{max} \\ V_{ch} &= 2 + 0.148\, R_2 \\ V_{dch} &= 1.926 + 0.124\, R_2 \\ R_{ch} &= [0.758 + 0.1309/(1.06 - R_2)]/S_{max} \\ R_{dch} &= [0.19 + 0.1037/(R_2 - 0.14)]/S_{max} \end{aligned} \tag{13}$$

where V_{ch}, V_{dch} = battery charge/discharge voltages, volts
R_{ch}, R_{dch} = battery charge/discharge internal resistances, ohm
S_{bat} = battery state of charge, Wh
S_{max} = the maximum battery state of charge, Wh.

Backup Power – Diesel Generator

The operation of a diesel generator is modelled as in Eq. (14):

$$P_{gen} = \begin{matrix} \text{constant, when operating} \\ 0, \text{ when stop} \end{matrix} \quad (14)$$

where P_{gen} is the generator power output which is determined by the generator rated power and its load factor. For the purpose of sizing, the generator model is not included in the simulation program. Instead, this model is used in the economic analysis of the backup system.

System Reliability Index

Cumulative loss of load hours over one year (LOLH) is chosen as the relevant index of the PV system reliability since this index can reflect well the cost of load shedding to consumers [8]. Moreover, this index has a relevant economic meaning because LOLH can be converted into the generator running hours, and the costs of backup power are then easily estimated.

Figure 3 illustrates the concept of LOLH. In this figure, $Z(t)$ represents "loss of load event" (LOLE) which is also a reliability index and has the mathematical form:

$$Z_{(t)} = \begin{matrix} 1, \text{ if load is shed} \\ 0, \text{ if load is met} \end{matrix} \quad (15)$$

It should be noted that "reliability" here is used to describe system unavailability due only to the lack of energy. The effects of failure of system facilities are not included. In other words, all system elements are assumed perfect within their respective lifetimes.

SIMULATION RESULTS AND SIZING PROCEDURE

The input of the simulation program includes load profile, array size (PVS) and battery capacity (BTYS). The output is the reliability index (LOLH) of the given input data under the local meteorological conditions. LOLF is given by the simulation too, but it is used to find the system performances only. The basic input/output arrangement and the support database of the simulation program are shown in Fig. 4.

The simulation outputs for load profile no. 1 (Fig. 2) at four array sizes and several battery capacities are depicted in Fig. 5. Figure 5 is a kind of presentation of the LOLH-PVS-BTYS relationship on an LOLH-BTYS map. But it is preferable to present the relationship in the form of iso-LOLH curves, i.e. the curves represent the combinations of PVS and BTYS which give the same LOLH values, so that the substitution between PVS and BTYS may be expressed clearly.

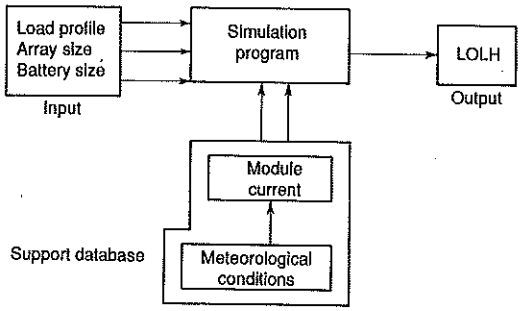

Fig. 4. Output, input and support database of simulation program.

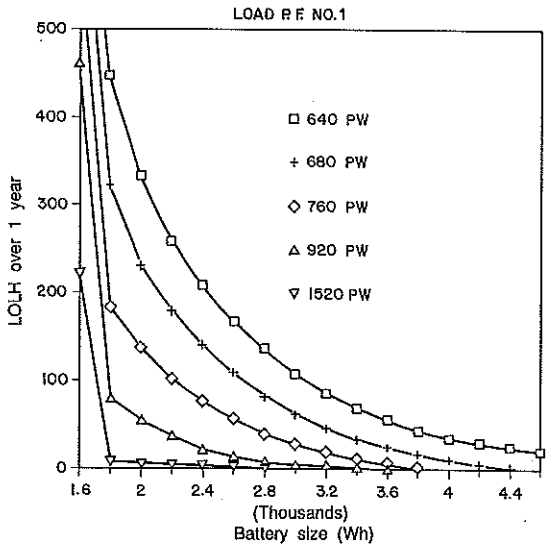

Fig. 5. Simulation results: LOLH versus BTYS at four array sizes for profile no. 1.

With "two-dimensional inverse interpolation" [9], the combinations of PVS and BTYS which result in the same LOLH value can be obtained from Fig. 5, and the combinations can be depicted on a PVS-BTYS map to make an iso-LOLH curve. Figure 6 shows the results when iso-LOLH curves for six LOLH values are drawn on the PVS-BTYS map. The data points obtained from inverse interpolation are depicted with legends, and the curves are their regression curves with the mathematical function:

$$f(X) = \exp\left(\sum_{i=0}^{6} a_i / X^1\right) \tag{16}$$

The parameters a_o, a_1, a_2,..., a_6 are calculated by transforming the fitted data against 1/X and Log(Y) scales and then using the polynomial regression technique. To fit all data points well is

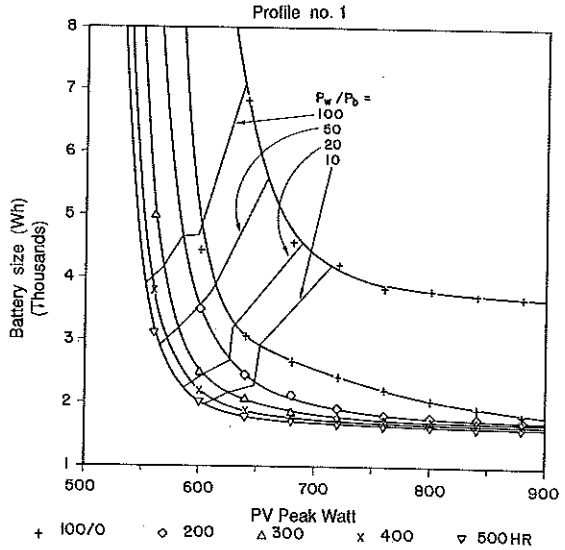

Fig. 6. Iso-LOLH curves, and optimum design points at four price ratios.

important because the slope of tangency of iso-LOLH curves is the key factor of sizing. Eq. (16) basically represents the analytical function of iso-LOLH curves although it is an approximation of simulation outputs.

Since iso-LOLH curves indicate that there exists many PVS-BTYS combinations meeting a prescribed reliability (LOLH), to find the particular combination leading to the least cost is preferable. Considering the iso-LOLH curve representing the LOLH value of R_o,

$$g\,(\text{PVS}, \text{BTYS}) = R_o \tag{17}$$

where g is the function representing an iso-LOLH curve.

The cost of purchasing arrays and batteries to meet reliability R_o is:

$$C = (P_w)\,(\text{PVS}) + (P_b)\,(\text{BTYS}) \tag{18}$$

where C = the total investment, US$
P_w = the array price, US$/peak watt
P_b = the battery price, US$/Wh
PVS = array size, peak watt (PW)
BTYS = battery size, watt-hour (Wh)

The problem becomes to

$$\text{MINIMIZE } (P_w)\,(\text{PVS}) + (P_b)\,(\text{BTYS})$$

$$\text{SUBJECT TO } g\,(\text{PVS}, \text{BTYS}) = R_o$$

The mathematical solution can be found through the method of Lagrange multiplier [10], and the Lagrange function is:

$$L = (P_w)\,(\text{PVS}) + (P_b)\,(\text{BTYS}) + m_L\,(g - R_o) \tag{19}$$

where m_L is the Lagrange multiplier. Differentiate Eq. (19) with respect to PVS, BTYS and m_L, and set the partial derivatives equal to zero, obtaining:

$$P_w + m_L\,[\delta g/\delta\,(\text{PVS})] = 0 \tag{20}$$

$$P_b + m_L\,[\delta g/\delta\ (\text{BTYS})] = 0 \tag{21}$$

$$g = R_o \tag{22}$$

Eq. (20) and (21) can be combined and written as:

$$-\,[\text{d(BTYS)} / \text{d(PVS)}] = P_w/P_b \tag{23}$$

The left of Eq. (23) is the marginal rate of substitution (MRS) between PVS and BTYS. It represents the rate at which PVS is decreased as BTYS is increased along the same iso-LOLH curve. Eq. (23) means that the minimum cost to meet reliability R_o occurs at the point where the MRS equals the price ratio P_w/P_b. Thus, the optimum point on an iso-LOLH curve is the point at which the negative of the tangency slope of the curve is equal to the price ratio.

Since the lifetimes for array and battery are different, the price ratio must reflect the real costs to the system. For instance, the array price is about 12 US$/peak watt and the battery price is about 120 US$/kWh. If arrays have a lifetime twice as long as that of batteries, the price ratio can be roughly taken as 50 (discount rate is ignored). Figure 6 also shows the optimum design points on each iso-LOLH curves for price ratio 100, 50, 20 and 10.

ECONOMIC ANALYSIS OF SYSTEM RELIABILITY

While it is clear that a higher degree of reliability requires higher investment in arrays and batteries, a lower degree of reliability results in a higher outage cost (i.e. the cost arising from lack of energy). Accordingly, trade-offs between system investment and outage cost must be evaluated to determine the optimum reliability. The cost of running a diesel generator is taken as the outage cost in this paper because it can reflect the cost to the PV system user(s) when the PV system is unable to supply energy due to unavailability of sunshine.

Table 2 lists the optimum combinations at six LOLH values for price ratio 50. The data are directly obtained from Fig. 6. Table 3 presents the assumptions for prices, lifetimes, inflation rate, discount rate, etc., for cost analysis. PV system cost, diesel generator running cost (including capital cost, operating cost and maintenance cost) and the total cost for each reliability level can thus be calculated from Table 2 and Table 3. The results are summarized in Table 4 and are shown graphically in Fig. 7. From Fig. 7 it can be seen that the reliability giving the least total cost occurs at LOLH = 354 hrs. This is the reliability which incurs the minimum cost so it is the optimum reliability for the assumed meteorological conditions and the load profile.

Table 2. Optimum sizes at price ratio 50 for profile no. 1.

LOLH (hr)	Array Size (peak watt)	Battery Capacity (watt-hour)
0	657	5566
100	611	3809
200	593	3455
300	581	3168
400	572	3019
500	565	2902

Table 3. Data for cost analysis.

PV array	
Cost	12 US$/PW
Life time	10 years
Maintenance cost	0 US$/year
Battery	
Cost	120 US$/kWh
Life time	5 years
Maintenance cost	0 US$/year
Diesel generator (including power distribution facilities)	
Rated power	1 kW
Load factor	50 %
Efficiency	2 kWh/litre
Capital cost	400 US$
Maintenance cost	5 % of the capital per year
Life time	7000 hours
Price year	the 0th year
Liquidation yield	0 US$
Diesel price	0.75 US$/litre
Discount rate	10 %
Energy escalation rate	4%
General inflation rate	4%

Table 4. Results of cost analysis.

LOLH	PV-Cap (1)	Gen-Cap (2)	Fuel (3)	Maintenance (4)	Total (5)
#0	9056.5	0	0	0	9056.5
##0	9056.5	400	0	20	9605.3
100	8134.4	400	18.75	20	8822.7
200	7843.8	400	37.50	20	8671.7
300	7639.4	400	56.25	20	8606.7
400	7500.0	400	75.00	20	8606.9
500	7391.3	400	93.75	20	8637.8

(1) Capital costs of PV arrays and batteries.
(2) Capital costs of the diesel generator.
(3) Diesel fuel cost in the first year.
(4) Diesel generator maintenance cost in the first year.
(5) Total costs.
* (1) – (5) in present value.
\# System without diesel set.
System with diesel set in spite of the zero LOLH value.

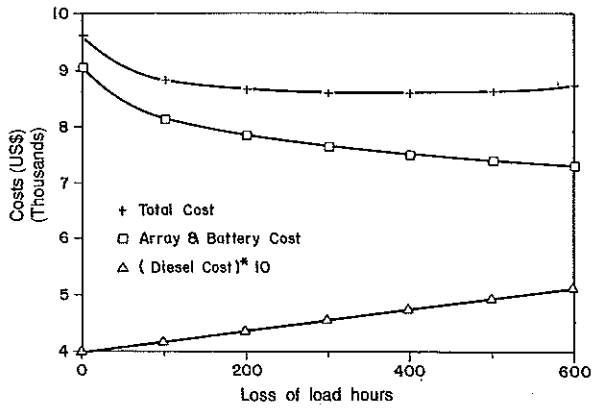

Fig. 7. Total cost, PV system cost and diesel generator running cost as a function of system LOLH.

The optimum combination of array size and battery capacity meeting the optimum reliability can be found by interpolating LOLH = 354 into Table 2 to find the corresponding sizes. They are approximately 576 peak watts and 3093 watt- hours.

Figures 8 and 9 show the investments in PV system, and operating and maintenance costs for the diesel generator. The sensitivity analysis is shown in Fig. 10. It indicates that capital cost is the most sensitive factor while diesel prices and inflation rate do not influence its energy cost significantly. It is therefore evident that to adopt a diesel generator in a PV system not only reduces the total cost but is also convenient for future demand growth because the marginal cost of supplying extra energy from a diesel generator is cheap.

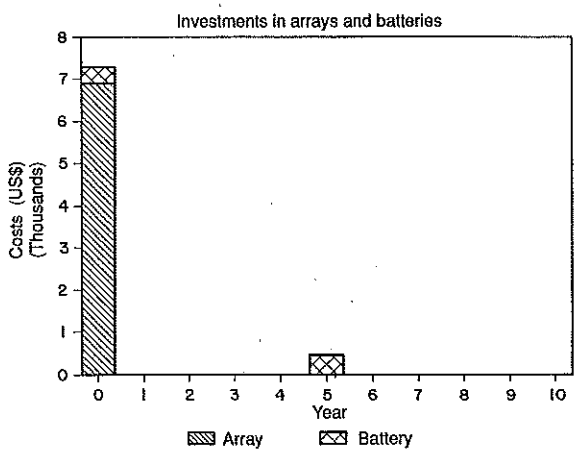

Fig. 8. Investments of PV system in arrays and batteries.

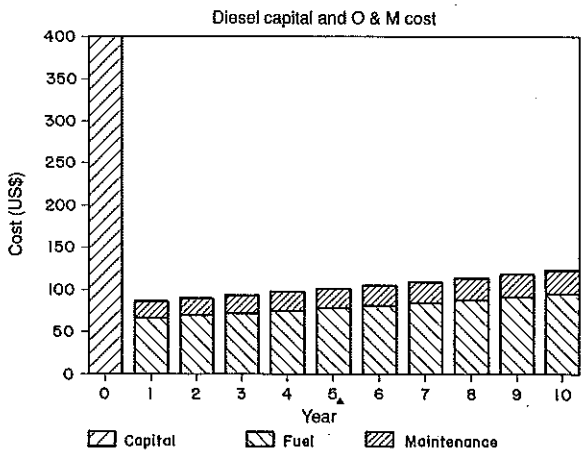

Fig. 9. Diesel generator capital, fuel and maintenance cost.

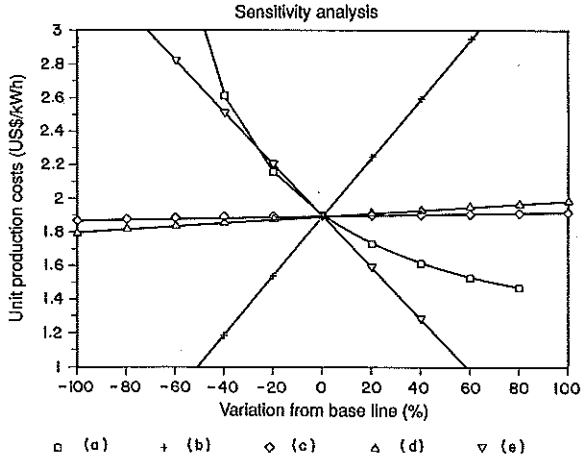

Fig. 10. Sensitivity analysis. (a) Lifetime, (b) Capital cost, (c) Inflation rate, (d) Diesel price, (e) Insolation.

DISCUSSION

Effect of Load Profiles on Sizing

Besides load profile no. 1, two more load profiles (no. 2 and no. 3 shown in Fig. 2) with the daily energy consumptions equal to that for profile no. 1 were also tested to find the optimum design points.

Figure 11 compares the sizing results (iso-LOLH curves) at LOLH=0 for the three profiles. It shows that the required BTYS and PVS are less for the load profiles fitting the solar radiation profile well. For instance, the cosine load profile with peak time at 12:00 (profile no. 3) fits the sunshine profile well so the required storage capacity and array size to meet LOLH=0 are the least among the three profiles tested.

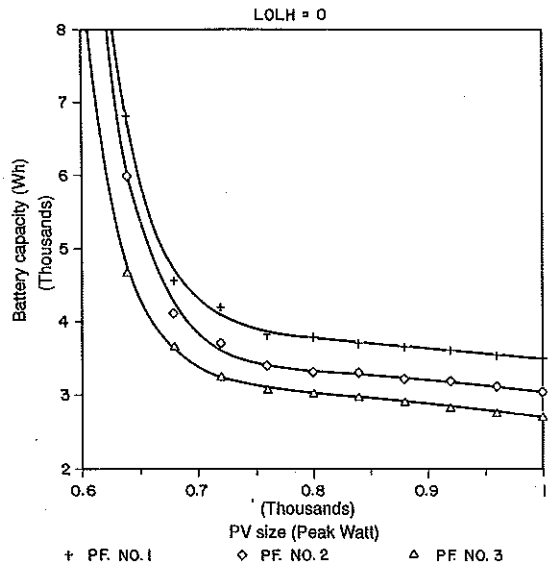

Fig. 11. Comparison of Iso-LOLH curves (LOLH = 0) for three load profiles.

The peak time (t_p) affects the sizing also. If peak demand occurs at noon, the required PVS and BTYS will be less. Figure 12 shows the variations of LOLH with peak time (t_p) for two PV systems; one is matched with the cosine load profile (profile no. 3), the other is matched with the profile no. 2. Both systems are designed to meet the condition of LOLH=0 if, t_p = 12:00.

It is clear that LOLH increases when t_p departs from 12:00. The effect of load pattern implies that load management is important for stand-alone PV systems because if some loads can be shifted from night to noon, the investment in array and battery can be reduced significantly.

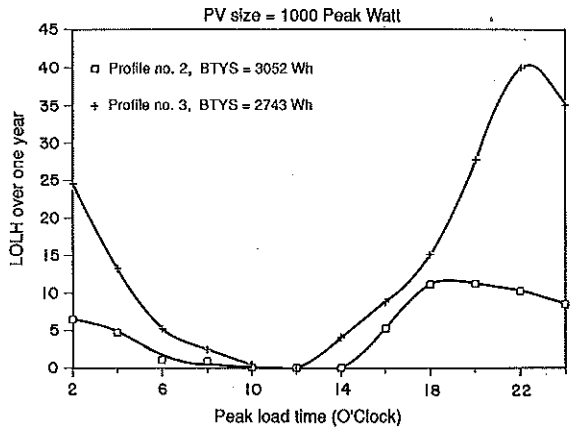

Fig. 12. Variations of LOLH with T for load profile no. 2 and no. 3.

Loss of Load Frequency (LOLF) and Battery Operations

Although all PVS-BTYS combinations on a iso-LOLH curve cause the same expected LOLH value, the corresponding loss of load frequencies (LOLF), i.e. the number of loss of load events (LOLE) in a given period, say one year, are quite different. For the systems with large PVS and small BTYS, the batteries have high charge/discharge rates so the average loss of load duration is short but LOLE occurs frequently. On the other hand, big BTYS and small PVS result in a low charge/discharge rate so the LOLE are characterized by their long duration. Thus for a certain value of LOLH, i.e. the sum of all durations of LOLE in a year, the system with small PVS and big BTYS have low LOLF, and the opposite designs have high LOLF. The relations of LOLF against PVS for 5 LOLH values are shown in Fig. 13. The battery capacities matching the PVS to cause the given LOLH values are not shown in the graph but can be obtained from Fig. 6.

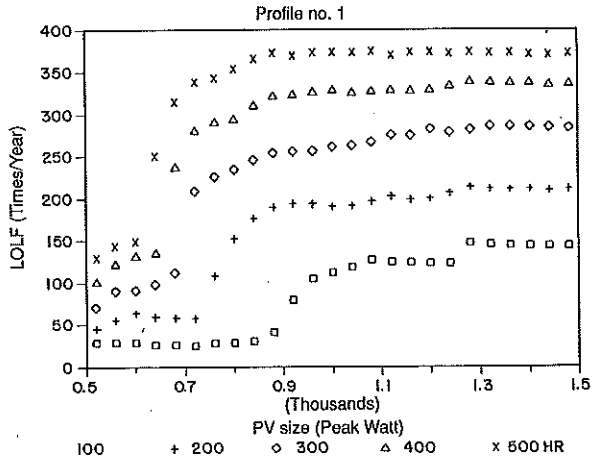

Fig. 13. Variations of LOLF with array sizes at five LOLH values.

In power system engineering, LOLF is an important reliability index because consumers are probably more sensitive to LOLF than LOLH. However, it is not important here because if a diesel generator is added to a stand-alone PV system (to charge batteries), LOLF can be controlled easily.

In addition to LOLF, the battery operation is also influenced by PVS-BTYS combinations. Because of the high charge/discharge rate of small BTYS systems, batteries discharge a high percentage of capacity each night and are recharged each daytime (if sunshine is available). This is the "deep cycle" operation. The shallow cycle systems are sized to use a small portion of the battery bank capacity each night. The big BTYS systems generally operate this way. Figure 14 shows the battery SOC variation over one year for three different designs to meet the LOLH = 0 condition. The tested profile is profile no. 1. Figure 14(a) shows a large BTYS system (PVS=560 PW, BTYS=48198 Wh). It can be seen from the graph that the system is a shallow cycle system. Each cycle uses about 5% of the battery capacity. Figure 14(b) (PVS = 1000 PW, BTYS = 3526 Wh) shows a deep cycle operation which consumes about 36% of the battery capacity each night. An intermediate case (PVS=680 PW, BTYS=4568 Wh) which uses about 26% of the capacity each night, is shown in Fig. 14(c).

Given the different battery operations (deep or shallow cycle), the type of battery selected is important. For instance, batteries with a low self-discharge rate are preferable for shallow cycle systems because the systems need to store energy for a long time. Deep cycle systems need batteries with a long cycle life, high depth of discharge and a high charge/discharge rate.

An important point which can be drawn from Fig. 14 is that battery capacity is not fully used, i.e. battery SOC is "floating" most of the time. Figure 14(a) shows that only on 11 days a year is the battery SOC lower than 60%. Again, Fig. 14(c) shows that only for about one-fifth of a year is the battery SOC lower than 70%.

As was explained previously, the systems are oversized to cover the few cloudy days which occur. If back-up power is introduced to cover the relatively low percentage of these cloudy days, the required battery capacity as well as array size can be reduced significantly and the investment will thus be less.

SUMMARY

The simulation approach to PV system sizing has been developed in this paper. It gives the optimum system reliability and the optimum combination of array size and battery capacity to meet the desired reliability. The conclusions of the study are summarized as follows:

(1) PV system's load profile influences its sizing significantly. Systems with load profiles similar to solar insolation profiles are preferable. Thus load management is important for PV systems to save initial investment and to assure the expected reliability.

(2) Iso-LOLH curves give the substitutive relationship between array and battery. Different PVS-BTYS combinations on an iso-LOLH curve have different LOLFs and battery operations (shallow cycle and deep cycle), so the price ratio of array prices to battery prices, which determines PVS-BTYS combination on the iso-LOLH curve, influences the type of battery used, i.e. shallow cycle and deep cycle.

(3) Since PV-alone systems are oversized to cover a relatively low percentage of cloudy days, the use of a diesel generator can reduce the investment in array and battery, and the hybrid PV/diesel systems usually have a total cost below that of PV-alone systems. From the viewpoint of future growth in demand, hybrid PV/diesel systems are also preferable.

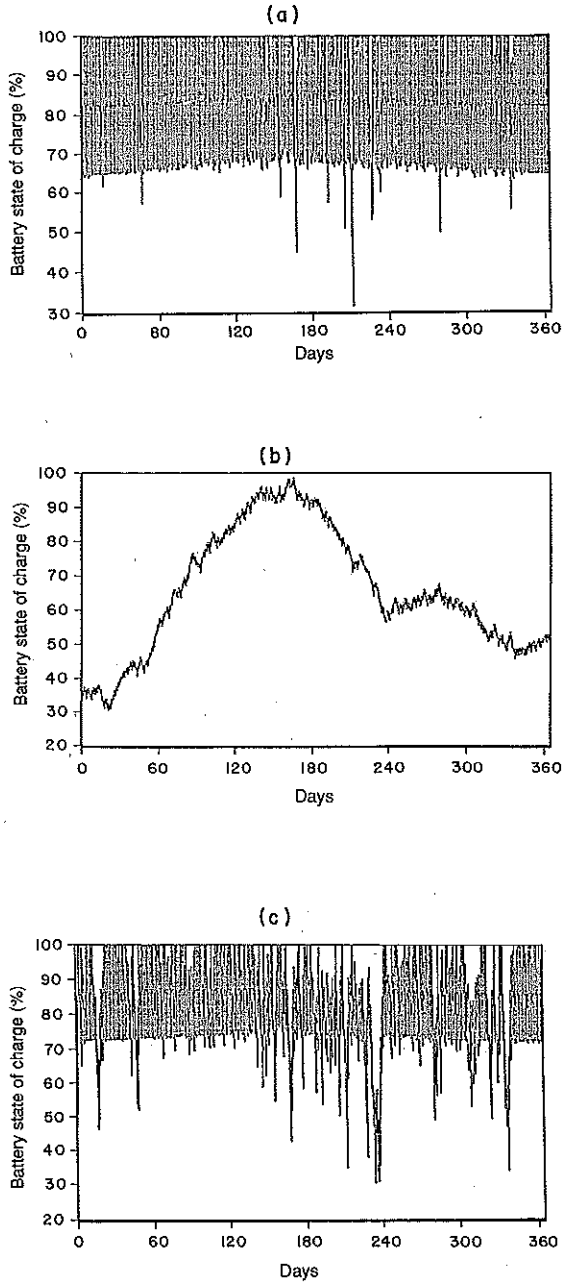

Fig. 14. Variation of battery SOC over one year.
(a) A deep cycle system
(b) A shallow cycle system
(c) A mediate case between (a) and (b)

LIST OF SYMBOLS

BTYS	battery size, Wh
C	cost of PV system, US$
D_m	amplitude of cosine function load profile, watt
D_s	battery self-discharge rate, watt
D_o	daily average demand, watt
$D(t)$	demand function, watt
E	daily energy consumption, kWh
$f(x)$	curve fitting function for iso-LOLH curve
g	analytical function of iso-LOLH curve
$H(t)$	function of cumulative loss of load hours
I_b	battery current, amps.
I	module current, amps
I_{mp}	module maximum-power current, amps
I_{sc}	module short-circuit current, amps
K_1	battery charge/discharge efficiency
K_2	battery charge/discharge resistance, ohm
K	ratio of peak demand to the lowest demand
P_w	the array price, US$/peak watt
P_b	the battery price, US$/Wh
PVS	array size, peak watt
R_{ch}, R_{dch}	battery charge/discharge internal resistances, ohm
R_o	reliability, hours
S_{bat}	battery state of charge, Wh
S_{max}	the maximum battery state of charge, Wh
$S(t)$	battery state of charge at time t, Wh
$T_a(t)$	ambient temperature at time t, °C
T_{max}	maximum ambient temperature, °C
T_{min}	minimum ambient temperature, °C
T_c	array temperature, °C
t_p	peak time, hr
V	module voltage, volts
V_{mp}	module maximum-power voltage, volts
V_{oc}	module open-circuit voltage, volts
V_w	the wind speed, m/sec
V	battery system voltage, volts
V_{ch}, V_{dch}	battery charge/discharge voltages, volts
$Z(t)$	function of loss of load event
α	the temperature coefficient of I_{sc}, amp/°C
β	the temperature coefficient of V_{oc}, volts/°C
ϕ	the incident solar insolation, W/m^2
θ_I	experimental constant related to insolation (W/m^2)$^{-1}$
θ_T	experimental constant related to ambient temperature (°C)$^{-1}$
θ_w	experimental constant related to wind speed (m/sec)$^{-1}$

REFERENCES

(1) Lasnier, France and Tony Gan Ang (1986), *Computer Package for Photovoltaic System Sizing, Design and Financial Evaluation,* Asian Institute of Technology, Bangkok.
(2) Exell, R.H.B. (1981), A Mathematical Model for Solar Radiation in South-East Asia (Thailand), *Solar Energy,* Vol. 26, pp.161-168.
(3) Chungpaibulpatana, Supachart (1981), *Model for Optimizing the Solar Plant Storage Tank Volume in Thailand,* AIT Thesis, No. ET-81-9, Asian Institute of Technology, Bangkok.
(4) Rauschenbuch, H.S. (1980), *Solar Cell Array Design Handbook,* Van Nostrand Reinhold Ltd., Toronto.
(5) Servant, Jean-Micheal (1986), Calculation of the Cell Temperature for Photovoltaic Modules from Climatic Data, *Proceedings of the 9th Biennial Congress of the International Solar Energy Society,* Pergamon Press.
(6) Hoover, E.R. (1980), SOLCEL II: An Improved Photovoltaic System Analysis Computer Program, *Proceedings of 14th IEEE PV Specialists Conference- 1980,* pp.1258-1261.
(7) Ang, Tony Gan (1984), *Analysis of a Compression Refrigeration Supplied by Photovoltaic Power,* AIT Thesis, No. ET-84-10, Asian Institute of Technology, Bangkok.
(8) Electrical Power Research Institute (1981), *Reliability Index for Power Systems,* EL-1773, Research Project 1353-1, U.S.
(9) Gerald, Curtis F. (1978), *Applied Numerical Analysis,* 2nd Ed., Addison-Wesley Publishing Co., U.S.
(10) Rao, S.S.(1984), *Optimization Theory and Applications,* Wiley Eastern Ltd., U.S.